Materials • Mechanics • Physiology • Engineering • Aerodynamics

BIKE TECH

Bicycling Magazine's Newsletter for the Technical Enthusiast

April 1985

Volume 4, Number 2

IN THE LAB

Biomechanics of Shifting Performance

Design of the Shimano New Dura-Ace Shifting System

Shinpei Okajima

In road racing, the performance of the bike's shifting system is the last thing on the rider's mind; except, of course, when the chain mis-shifts at a critical moment or jumps off the chainwheel entirely. Such failures are not uncommon—there were even a few instances of jumped chains in the 1984 Olympic cycling events in Los Angeles. Beyond these catastrophic failures, conventional shifting components impose other demands on the racer: the need to ease pedaling force during the shift, and the need for precision in moving the shift lever. The racer must devote at least some of his attention and energy to these demands to avoid mishaps. And it's generally agreed that shifting becomes more of a problem when the racer is tired or riding on rough terrain.

The New System

In this study we took extensive laboratory measurements of both the mechanical and biomechanical performance of the shifting system. In particular, we wanted to compare the Shimano New Dura-Ace system against a conventional derailleur/shift-lever combination. The New Dura-Ace group uses the Shimano Index System (SIS) shifting mechanism, and includes the following components:

—*shift levers* (SL-7400): A ratchet-and-pawl type of mechanism ensures each movement of the lever produces a precise and repeatable amount of displacement in the shifting cable. The mechanism transmits

Shinpei Okajima is Assistant Manager of the Development Section in Shimano's Technical Division in Osaka, Japan. One of his major projects has been the development of Shimano's "New Dura-Ace" line of components including the "indexed" shifting system, described here, and the braking system, to be described in a future issue of Bike Tech.

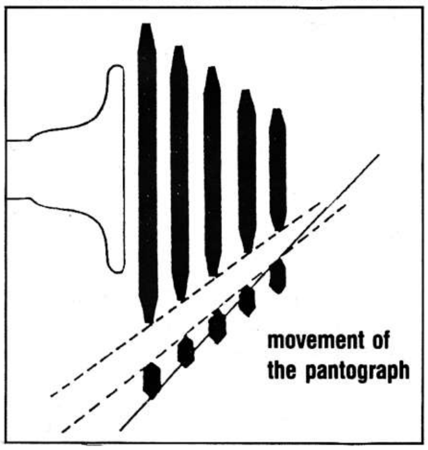

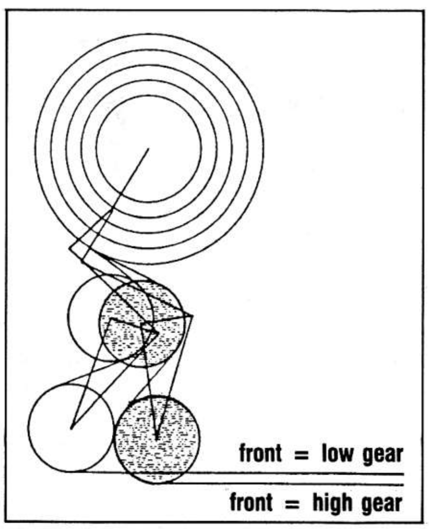

Figure 1: For precise shifting, the distance from the derailleur jockey pulley to freewheel sprocket teeth should be small and also constant in all gears.

IN THIS ISSUE

an audible and tactile click when the shifting motion is complete. (The levers can also be used in the conventional "friction" mode by turning a tensioning knob to disengage the ratchet index mechanism.)

—*rear derailleur* (RD-7400): The mechanism was designed with a single parallelogram to keep the guide pulley at a constant distance from the sprocket teeth in all gears. Thus, the amount of cable displacement needed to produce a shift remains the same throughout the shifting range. (The derailleur will handle 12T to 26T sprockets, and has a 26T take-up capacity.)

—*multi-freewheel* (MF-7400-6): An improved cassette-body based on the Dura-Ace freewheel carries 6 sprockets in the 13T to 32T range. Also, a new freehub (FH-7400, 12T to 32T range) was designed, which can be used with existing Dura-Ace sprockets.

—*front derailleur* (FD-7400): A specially-shaped chain guide, with a "creased" inner plate and a bridge at the front, provides better control of the chain during shifting.

—*chainwheel* (FC-7400): Improvement in the tooth shape of the gear provides better contact with the chain.

—*outer casing for shifting cables:* Designed for use with any conventional inner cable.

Any chain normally used in racing (Uni-Glide or narrow Sedis type) can be used with the New Dura-Ace system. Our tests used the Sedi Sport chain, since this more flexible chain is somewhat harder to shift than the Uni-Glide.

BIKE TECH

Executive Editor
Robert G. Flower

Technical Editors
Hal Jeffrey Davis
Jim Redcay

Managing Editor
Susan Weaver

Contributing Editors
Fred Delong
Gary Klein
David Gordon Wilson

Editor Emeritus
Crispin Mount Miller

Circulation Manager
Pat Griffith

Chairman
Robert Rodale

President
Robert Teufel

Publisher
James C. McCullagh

Copy Editor/Proofreader
Cheryl E. Kimball

Art Director
John Lenaas

Assistant Art Director
Catherine L. Schwartz

Illustrator
George Retseck

BIKE TECH (ISSN 0734-5992) is published bimonthly by Rodale Press, Inc., 33 E. Minor St., Emmaus, PA 18049. Subscription rates: United States, one year $14.97; two years $29.94; Canadian add $3.00 per year, payable in Canadian funds; other foreign add $6.00 per year for sea mail, $10 for air mail, payable in U.S. funds. Single copy price: $2.50. Inquire about bulk rates.

POSTMASTER: Send address change to *Bike Tech*, 33 E. Minor St., Emmaus, PA 18049. Second-Class Postage Paid at Emmaus, PA 18049. *Bike Tech* may not be reproduced in any form without the written permission of the publisher.

The "conventional system," which is referred to in all of the following comparison tests, consisted of the following:

—shift levers: Campagnolo Record downtube levers

—rear derailleur: Campagnolo Super Record

—freewheel: Regina CX, normal spacing

—front derailleur: Campagnolo Super Record

—chainwheel: Campagnolo Super Record

—chain: Sedis Sport

This particular group was selected to represent the best high-performance components of *conventional* design that are normally used in road racing.

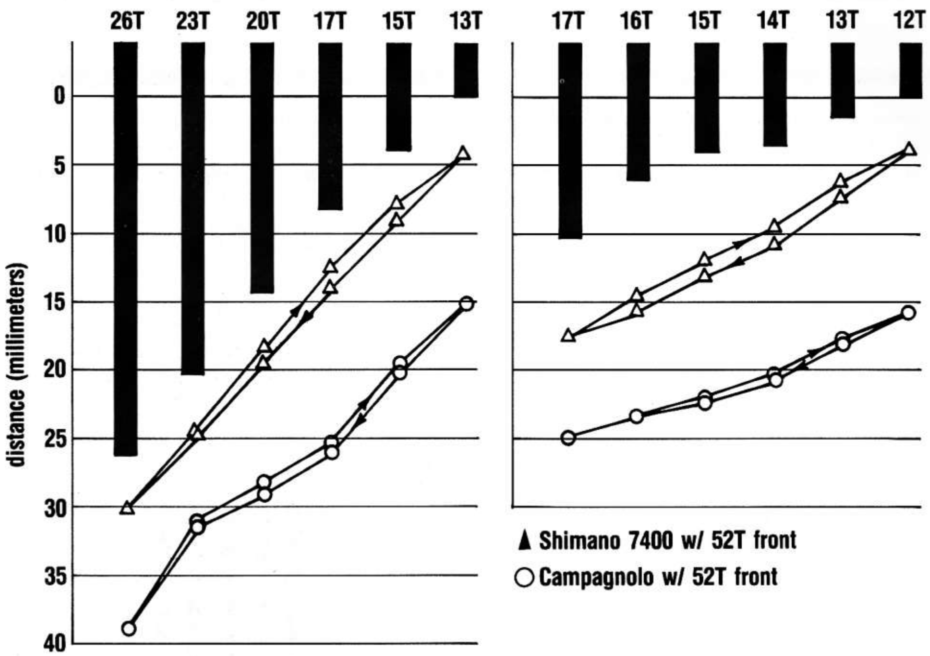

Figure 2: Actual measured distances from jockey pulley to freewheel sprocket teeth for New Dura-Ace 7400 and Campagnolo Super Record derailleurs, used with two different freewheels (13T-26T and 12T-17T).

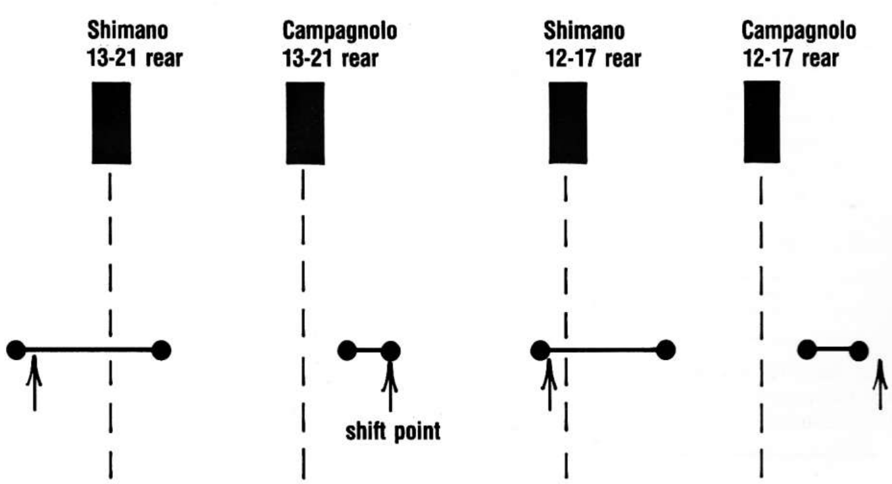

Figure 3: Rear derailleur performance: operating range of Shimano versus conventional model while downshifting with 52T chainwheel. Solid circles indicate the start of the "chatter zone"; line joining the circles is the chatter-free zone. Arrow indicates the point where shifting occurs. Data are averages of the 5 downshifts in the 21T-13T range (at left) and the 17T-12T range (at right).

Rear Derailleur Design

For quick and accurate shifting performance, the most critical design parameter is the distance from derailleur jockey pulley to freewheel sprocket teeth. With conventional derailleurs, the problem is that shifting under load often requires "overshifting," with a subsequent adjustment of the shifting lever to stop the chattering noise. To avoid this problem, we attempted to make the pulley-to-sprocket distance as *short* as possible, so that shifting will occur early regardless of loading on the pedals. In addition, we wanted to keep this distance *constant* at all gear settings, both front and rear, so that the ratchet mechanism of the SIS shift lever would work properly (see Figure 1).

These requirements led us to use a single slanted parallelogram and a single pivot axis in the rear derailleur (RD-7400) design. Measurements show that this design achieves a shorter and more constant pulley-to-teeth distance than the conventional derailleur (see Figure 2). As a result, the point at which shifting occurs during the shift-lever movement is relatively constant regardless of pedal loading and front chainwheel size (see Figure 3).

Shake Out

Regardless of design, durability of derailleurs in road racing has always been a problem. Products that could be used for years by casual tourists must be replaced weekly or monthly when used on muddy cyclo-cross or cobblestone road race courses. To simulate these conditions in the lab, we built an "endurance test facility" (see Figure 4). Here the complete drivetrain is subjected to muddy water spray plus severe mechanical vibrations (frequency is 12 to 14 Hz) while carrying the full pedaling load.

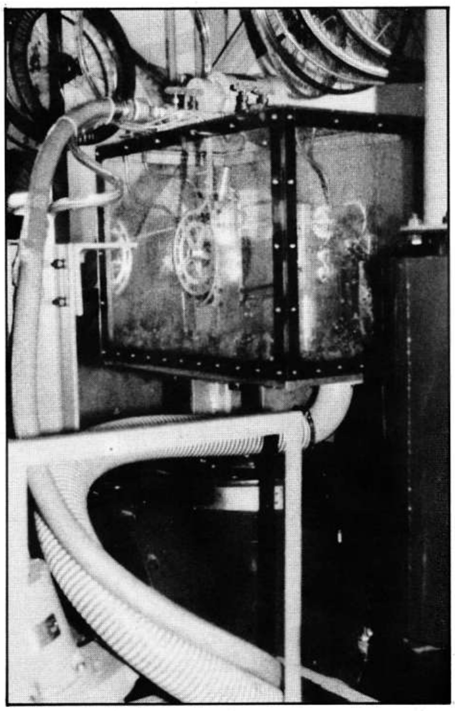

Figure 4: Endurance test chamber.

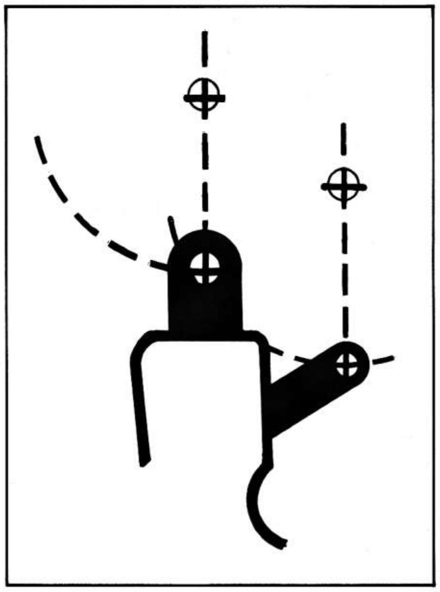

Figure 5: Cross-section (from front) of chain guide of New Dura-Ace front derailleur. Crease in inner cage plate ensures single-point contact with chain.

The conventional derailleur system could withstand an average of 72 hours of this abusive treatment before the high-end shift (13T to 14T) became unreliable. (This represents about one year of continuous use in professional road racing.) We took this value as the performance target which the New Dura-Ace design would have to meet or exceed. Testing of prototypes on the endurance machine, plus field trials in Holland, showed us that the following construction features provided improved durability:

—rubber ring seals on pivot axle, bracket axle, and parallelogram axles
—brass bushings on parallelogram axles
—titanium carbide coating on pulley bushings
—stainless steel teeth on jockey pulley.

With these features, the New Dura-Ace derailleur remained functional on the endurance tester approximately three times as long as the conventional derailleur.

Front Derailleur Design

The two factors in front derailleur design that are most important for efficient shifting are:

—*control of chain position*: In upshifting, a large force must be exerted on the chain to lift it, against the chain tension, onto the larger chainwheel. With conventional designs, the derailleur itself must exert this force; the result is either the need for large forces on the the shift lever, or the need to reduce chain tension (by unloaded pedaling) until the chain catches on the larger gear. The New Dura-Ace design takes a different approach: the necessary upward force is obtained by redirecting the motion of the front chainwheels. This is achieved by forming the inner cage plate with a specially-shaped "crease" (see Figure 5). The crease stiffens the cage plate and, more importantly, makes only single-point contact with the chain (unlike conventional flat chain guides), thus guiding the chain along a prescribed path (see Figure 6). The end result is that considerably less force is needed on the shifting lever with the new system (Figure 7). An additional benefit of the new design is that the stroke (distance of lever travel) needed to shift is also reduced (Figure 8).

—*range of adjustment*: Conventional front derailleurs are designed with a fairly nar-

Figure 6: Two phases in upshifting with New Dura-Ace front derailleur.

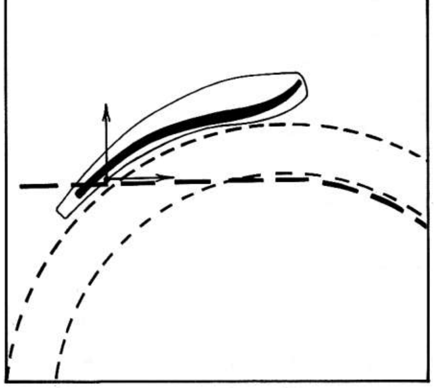

a) When inner cage plate first contacts the chain, friction between the two develops a reaction force which serves to lift the chain onto the larger gear.

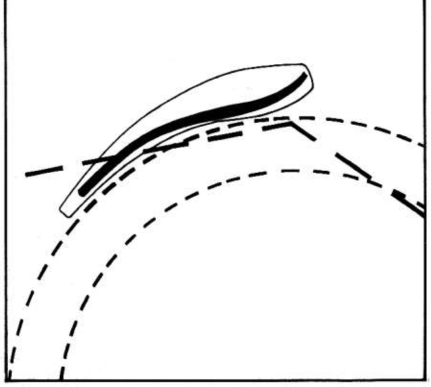

b) The point of contact between chain and cage plate follows contour of the "crease."

Figure 7: Front derailleur performance: tension force in derailleur cable (measured by in-line strain gauge) in a 42T - 52T upshift, for both unloaded and loaded pedaling conditions. The torque load for the front derailleur tests in Figures 7 and 8 is applied with a motor and electric brake, with the pedaling cadence set at a constant 100 RPM. In the labels for Figures 7 and 8, the "full" torque load (30 kg-cm = approximately 26 inch-lb) is measured at the axle of the rear wheel. Note that, with the Shimano system, force in the derailleur cable is lower for both loaded and unloaded pedaling

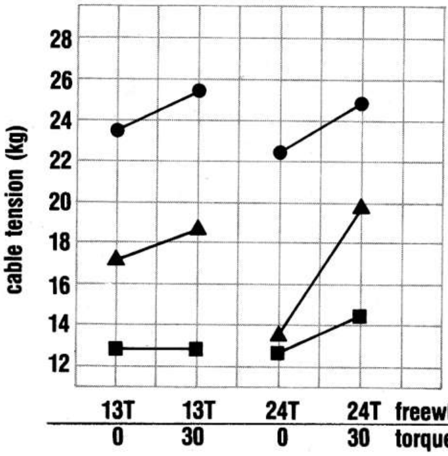

Figure 8: Front derailleur performance: measured stroke (mm) of derailleur movement required to shift. The torque load is measured at the rear wheel axle, and the pedaling cadence is a constant 100 RPM.
Note that in all cases but one, the Shimano derailleur shifted with the shortest stroke.

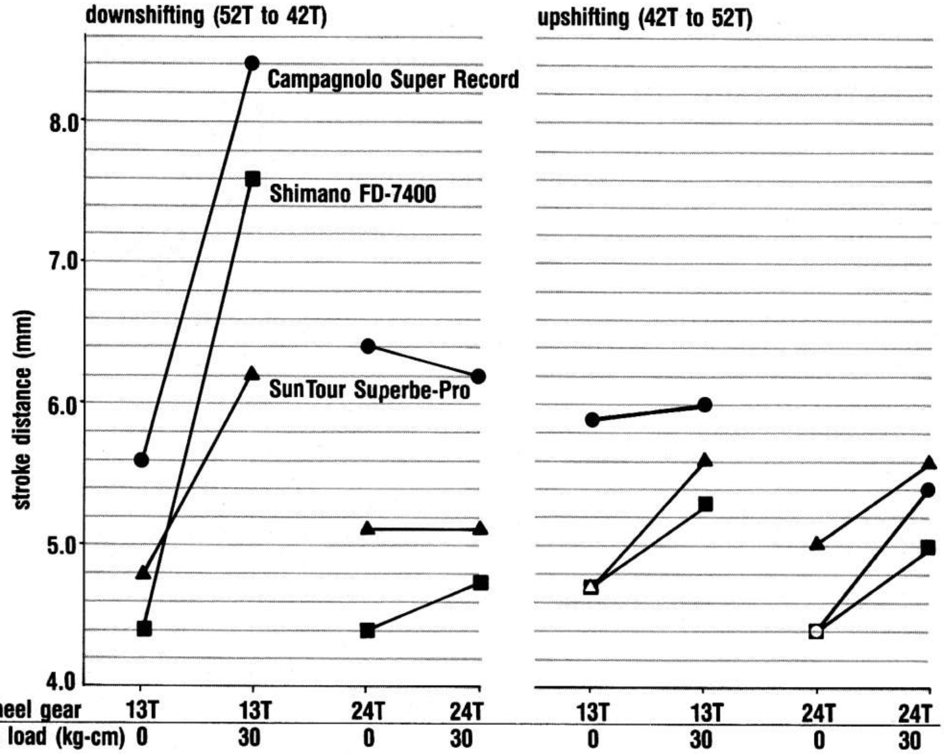

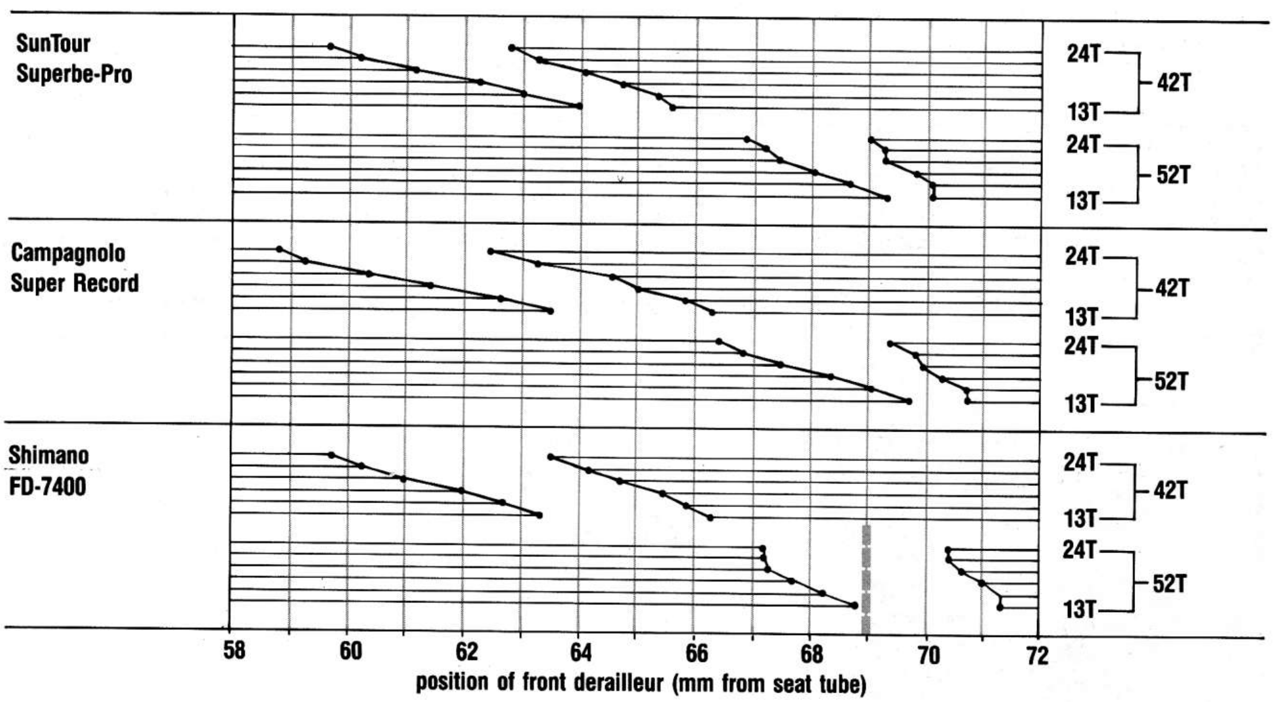

Figure 9: Adjustability range of 3 front derailleurs: for all possible front and rear gear combinations, this chart shows the position of front derailleur at which "interference" (ie, chain rubbing on chain guide) just begins to be detected. (Position is measured in millimeters from outside edge of seat tube to inside edge of outer cage plate). Example: when the Shimano front derailleur is located at 69 mm distance (dashed line), then the full range of 6 freewheel gears can be used without need for readjustment. For the Campagnolo and Sun-Tour derailleurs, there is no position of the front derailleur that allows all 6 freewheel gears to be used without some readjustment needed. (Freewheel gears are 13/15/17/19/21/24.)

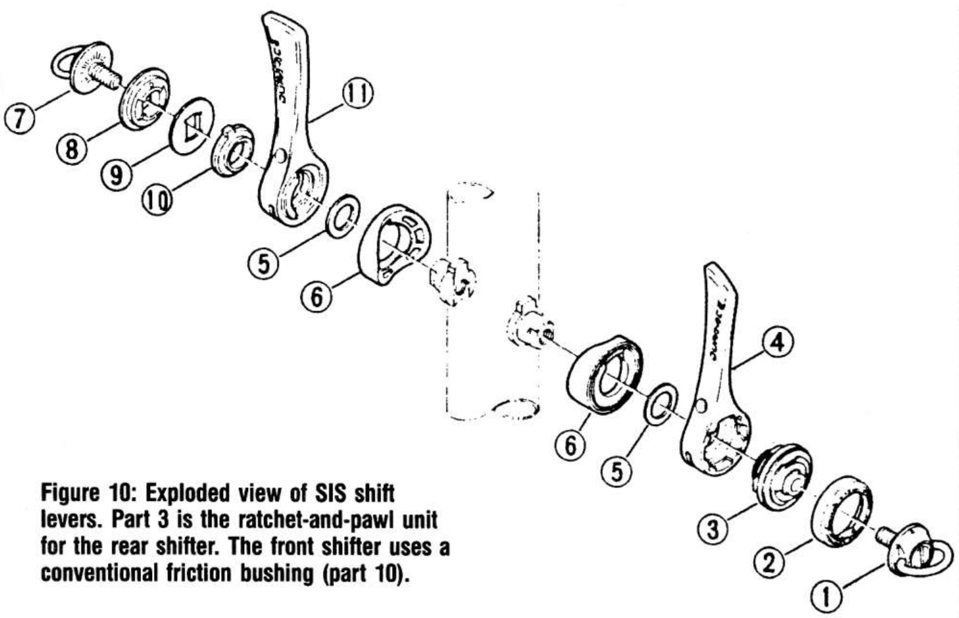

Figure 10: Exploded view of SIS shift levers. Part 3 is the ratchet-and-pawl unit for the rear shifter. The front shifter uses a conventional friction bushing (part 10).

row gap between inner and outer cage plates, in order to prevent late shifting. The drawback to the narrow gap is that the rider must re-adjust the front derailleur after shifting only 2 or 3 gears on the rear. With the New Dura-Ace design, a relatively wide gap between the cage plates is possible because the "creased" and contoured chain guide provides the necessary control of chain position. The end result is that a wider range of freewheel gears may be covered without need for readjusting the front. (see Figure 9).

Shift Lever Design

The shift lever is the main interface between the rider and the derailleur. Our biomechanical testing (described below) showed that shifting with conventional derailleurs is a fairly complex process that resembles a feedback control loop. The rider first grasps the lever and moves it a certain distance. Then the rider waits for a whole series of feedback signals (eg: sound, lever torque, and pedal force) to determine if the lever needs to be moved farther forward or back. After making these adjustments, the rider can let go and continue riding. The time required for this feedback process is about 0.77 seconds with conventional derailleurs.

If the rider could simply hit the lever in one rapid arm motion, with no need to linger for fine adjustments, then shifting would be quicker and would require less attention and energy. The Shimano Index System was designed to meet this goal, specifically by eliminating the need for feedback control. A ratchet-and-pawl mechanism is incorporated into the pivot of the rear shift lever (see Figure 10). A quick push against this lever will move the derailleur cable a precise distance, for a positive shift, and a built-in stop will prevent overshifting. This action is essentially open-loop or "ballistic" control, and takes less than half as much time, by our measurements, as conventional shifting.

The SIS lever can also be operated as a normal friction-type shifting lever for use with non-Dura-Ace freewheels. The changeover is made quickly by a half-turn of the cover of the ratchet unit (part #1 in Figure 10). This changeover feature will be useful if racing conditions call for quick replacement of the rear wheel.

Durability of the shifting lever was evaluated using the muddy-water endurance tester described above. Results showed that the ratchet assembly has a lifetime of about 300,000 shifts (about 600 days of professional road racing). Replacement of the unit is needed when the teeth or pawl become worn and indexing becomes unreliable.

Photo courtesy of Shimano

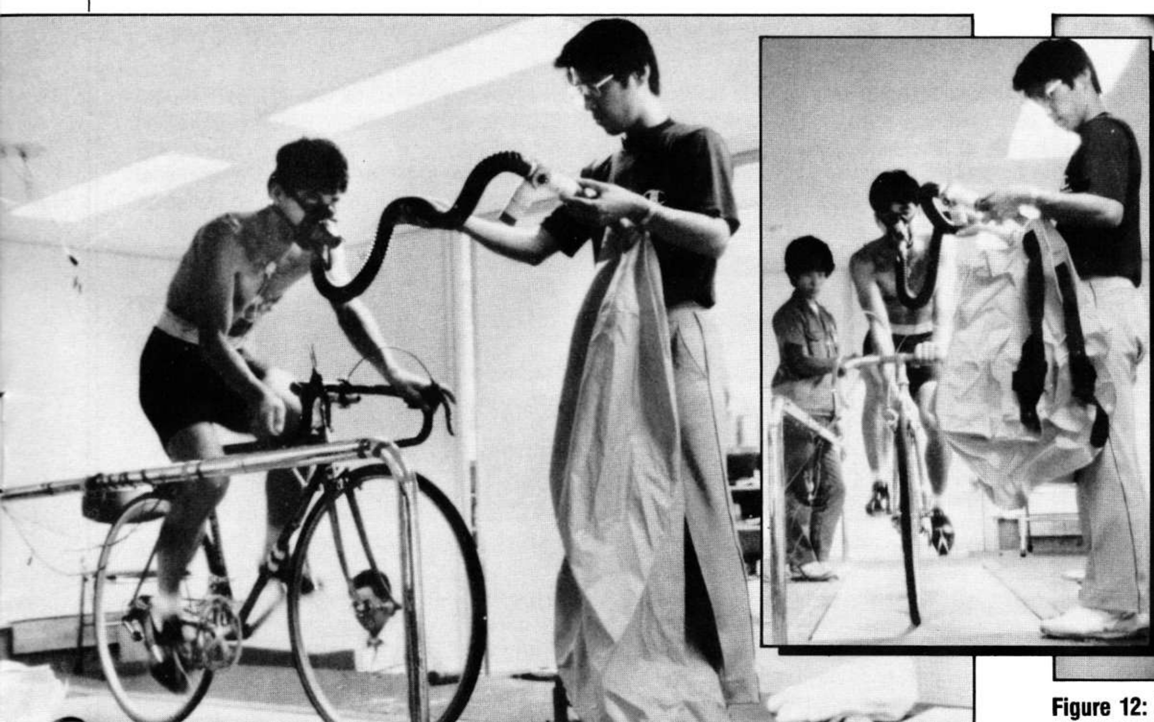

Figure 11: Two views of the instrumented test bike on treadmill with rider wearing respiratory gas sampler plus electromyographic sensors.

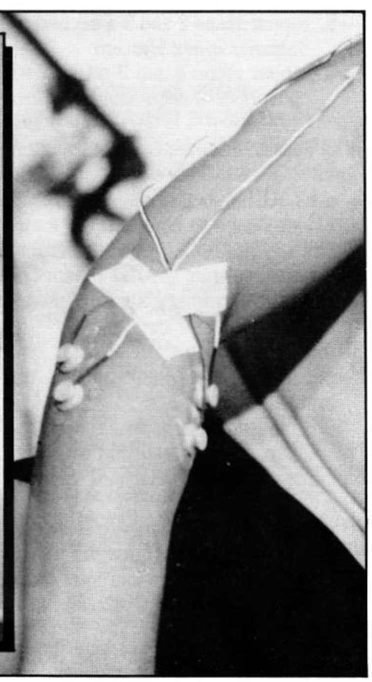

Figure 12: Electromyographic sensors on rider's upper forearm record the actions of flexor (on left) and extensor (on right) muscles in shifting.

Biomechanics - The Bottom Line

Does it really require less effort to shift with the Shimano Index System? We answered this question by means of a direct physiological test. We found, in short, that the test riders' oxygen consumption was 3 to 6 percent *lower* with the SIS system, compared to a conventional derailleur shifter, and with all other conditions (pedaling speed and torque, etc.) held constant. Here is how the tests were done.

Three experienced amateur bicycle racers were the subjects. The basic plan called for the test riders to shift the rear derailleur every 5 seconds (from 17T to 19T and back again) while riding a treadmill at a controlled speed (24 km/hr = 14.91 miles/hr) and work level. Before the study, the subjects trained to become accustomed to treadmill riding. For the study, each subject proceeded through the following sequence:

—1. brief warm-up period of road riding
—2. 5 minutes rest (sitting)
—3. treadmill riding on bike with conventional derailleur system:
  a. 3 minutes at 2 percent grade
  b. 3 minutes at 3 percent grade
  c. 3 minutes at 4 percent grade
  d. 3 minutes at 5 percent grade
—4. repeat steps 2 and 3 on bike with Shimano Index System
—5. repeat steps 2 and 3 a second time with Shimano Index System
—6. repeat steps 2 and 3 on bike with conventional derailleur system.

The bike and rider were instrumented as follows:

—a KUREHA brand gas analyzer (Figure 11) was used to continuously monitor respiratory gas for oxygen and carbon dioxide
—electromyogram (EMG) sensors placed on the rider's primary shifting muscles (Figure 12)
—touch sensor on the rear shift lever
—strain gauge on seat tube near bottom bracket
—tachometer on rear wheel

All readings were recorded by a digital data recorder and later analyzed by minicomputer.

Graphs of typical data are shown in Figure 13. The differences between the Shimano SIS components (upper graph) and the conventional components (lower graph) are striking:

—EMG activity is much lower with the SIS system, indicating that less muscle action is expended
—lever stroke is more definite with the SIS system, indicating that little overshoot or hunting occurs

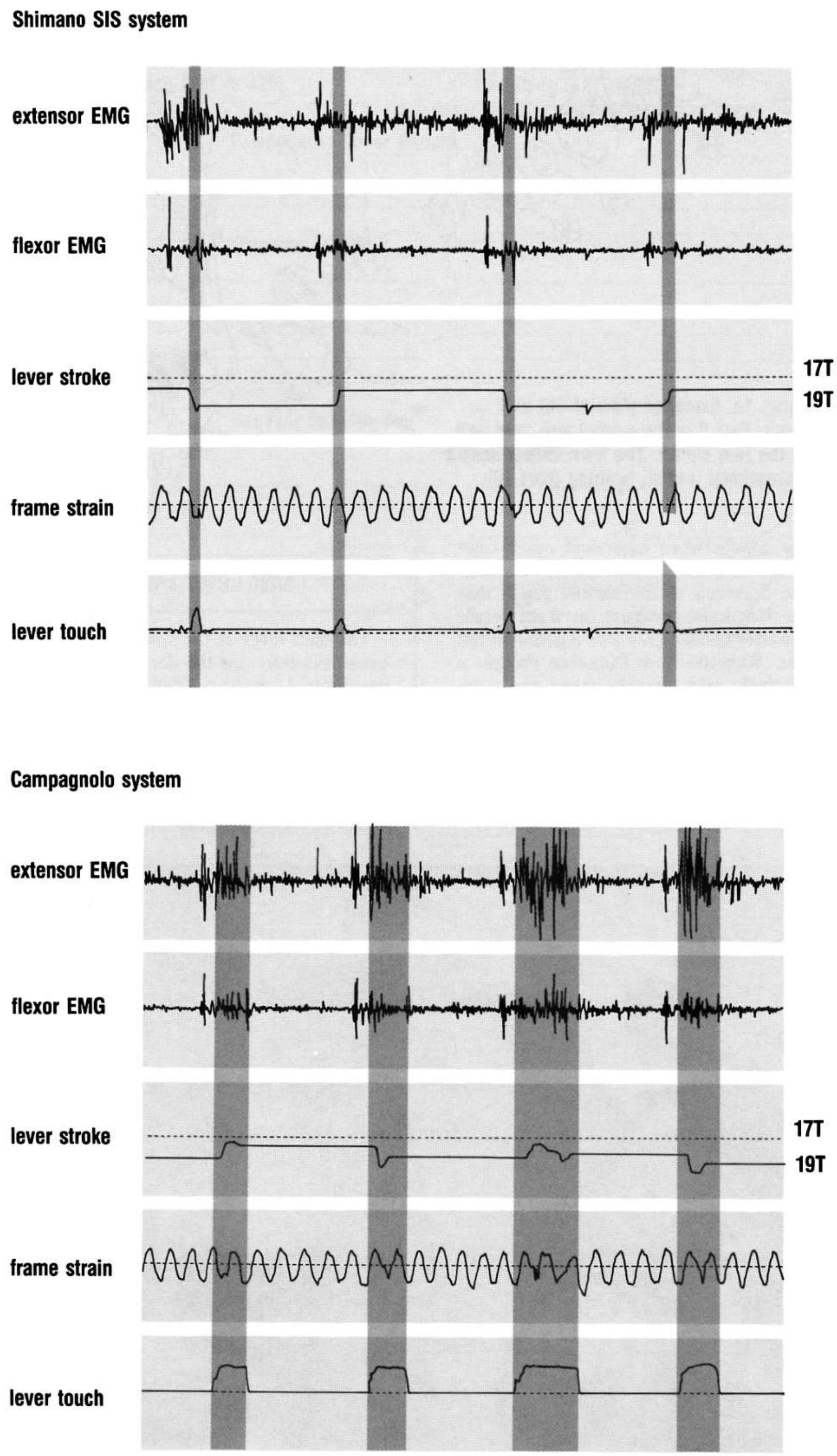

Figure 13: Typical biomechanical data recorded during a 20-second time interval with the Shimano system (upper) and Campagnolo (lower). Shaded vertical areas indicate the lever touch period as measured by the touch sensor.

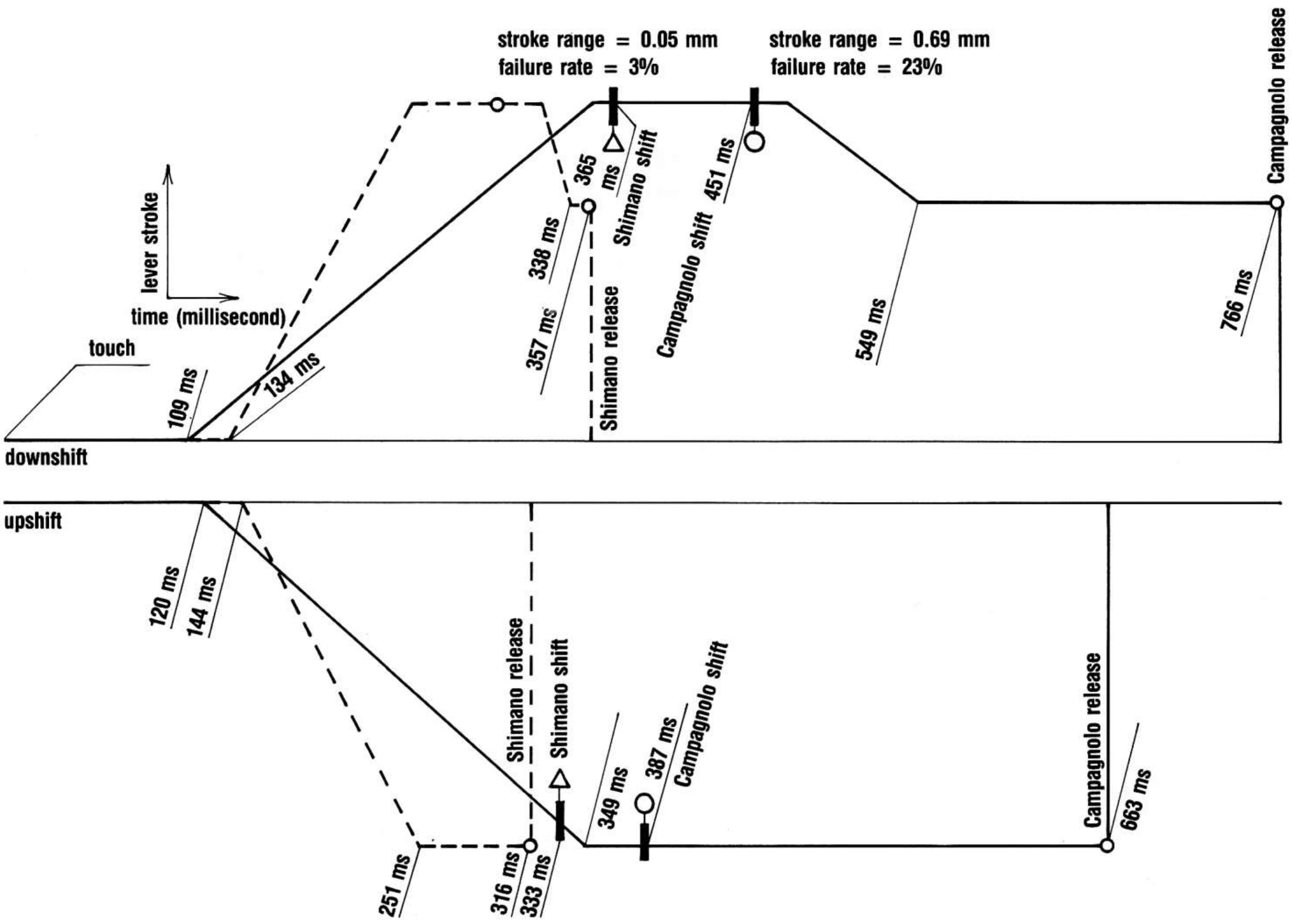

Figure 14: Statistical summary of lever-stroke versus time for shifting with Shimano system (dashed lines) and conventional system (solid lines). Upper graph shows downshifting (17T to 19T), lower graph shows upshifting (19T to 17T). Times (milliseconds) plotted on the graphs are averages of 36 shifts, for one subject riding at 24 km/hr on the treadmill. In all cases, the time = 0 point is defined as the instant when subject first touches the lever. The "release" point is the instant when subject lets go of lever. "Range" means the 3-sigma standard deviation of the sample. "Failure rate" is defined as the percentage of mis-shifts that occurred in the trials.

—lever touch period is shorter with the SIS system, indicating that shifting occurs quicker and more positively
—frame strain measurements show much smoother application of power with the SIS system, indicating that pedaling force is smoother and less disrupted than with the conventional components.

A statistical summary of the data on lever touch versus time is shown in Figure 14. Upper graphs show downshifting performance (17T to 19T); lower graphs show upshifting performance. Again the differences between Shimano and the conventional system are striking:
—the SIS lever reaches its maximum displacement much quicker than the conventional lever
—actual shifting occurs sooner with SIS system: for downshift, 365 ms with SIS versus 451 ms with Campagnolo; for upshift, 333 ms with SIS versus 387 ms with Campagnolo
—rider releases the lever over twice as soon with SIS system: for downshift, 351 ms with SIS versus 766 ms with Campagnolo; for upshift, 316 ms with SIS versus 663 ms with Campagnolo
—with the SIS system on both down and upshift, the rider releases the lever *before* shifting action of the chain is actually complete
—the four results just mentioned lend strong support to our hypothesis that the Shimano system operates by means of open-loop "ballistic" control, compared to the slower closed-loop feedback type of control needed for the conventional derailleur
—on downshifting, the Shimano system produced only 1 mis-shift out of 36 trials (3 percent failure rate), while the conventional system produced 8 mis-shifts (23 percent failure rate).

The bottom line in designing components for racing is better performance. To obtain a laboratory measurement that could reliably predict racing performance, we used oxygen consumption to indicate the rider's level of effort. The result, shown in Figure 15, demonstrates that the Shimano shifting system produces a measurable savings in rider effort. At a power level equivalent to climbing a 3 percent incline, the rider's oxygen consumption was only 2.04 l/min with the SIS system, compared to 2.17 l/min with the conventional system, a savings of about 6 percent. Statistical analysis shows that this difference is significant at the 95 percent

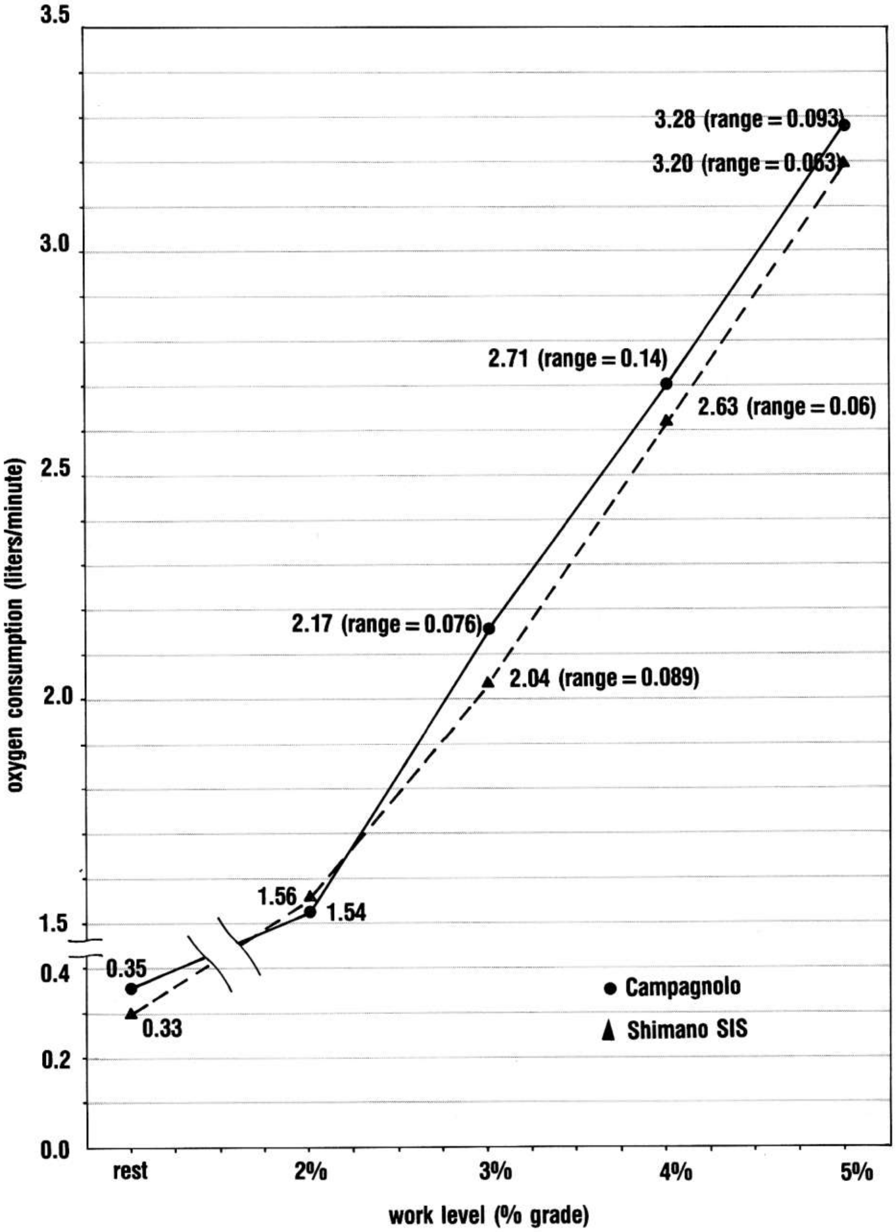

Figure 15: Oxygen consumption versus work level for shifting with Shimano system versus conventional system. Riding speed was 24 km/hr on treadmill, with shifting (from 17T to 19T and back) every 5 seconds. Averages of 7 trial runs with one subject are plotted. "Range" means the 3-sigma standard deviation of the sample.

confidence level (i.e., there is less than 5 percent probability that this difference could arise by random chance). For climbing the 4 percent and 5 percent inclines, savings with the SIS system are on the order of 3 percent, and this is statistically significant at the 75 percent level.

The meaning of these results is clear: the physiological load imposed on the rider is significantly lower with the New Dura-Ace system compared to the conventional system, under conditions of moderate hillclimbing and frequent up/down shifting. It is very likely, in our view, that this savings in shifting effort will translate into better competitive performance under real racing conditions.

BOOK REVIEW

Goldberg's Variations

The Spoking Word

Leonard Goldberg
published June 1984,
approximately 200 pages
$11 postpaid ($16 Canadian)
from:
Cascade Bicycle Products
PO Box 2548
Bellingham, WA 98227
(also available in retail outlets)

reviewed by Hal Jeffrey Davis

We certainly do take bicycle wheels for granted. Even wheelbuilders don't usually give much thought to the delicate balance of forces that keeps our wheels in line. For people who long to understand the theory behind wheel spoking patterns, here is a new book that you should read. **The Spoking Word** by Leonard Goldberg sheds new light into the tradition-bound world of wheelbuilding, and contains a wealth of insights and surprising new ideas.

The book's major topic is the design of wheel spoking patterns. Goldberg takes the classical engineering approach to the problem: he sets up the physical equations which relate forces within the wheel to the wheel's geometry and usage conditions. He then solves these equations to find the forces and stresses exerted on the wheel rim, hub, and spokes. With these solutions in hand, he offers recommendations for improved spoking patterns, for longer spoke life, less flex, et cetera.

What makes this book important is that it's not merely an academic exercise: Goldberg has plied the wheelbuilder's trade for the past eight years in his own bike shop, and his experience clearly shows through. Moreover, prior to wheelbuilding, Goldberg was a design engineer at the Boeing Airplane Company. The book itself grew out of a series of courses taught by Goldberg at Green River Community College and Northwest Free University, both in Washington state. You can imagine that Goldberg has heard almost every question that can possibly be asked about wheel design. He has tried to put all of his answers into this book.

It's true that the algebraic formulas and tables of numbers that fill the pages of **The Spoking Word** do look intimidating at first. But the persistent reader will quickly find that nothing more than high-school trigonometry, algebra, and physics is involved. In fact, the book is so well-organized, with most of the derivations relegated to appendices, that the non-math reader could glean many of Goldberg's insights on first reading. I will admit, however, that I had to rely on a pocket calculator and scratchpad to keep track of some of the discussions. This is most likely due to the high density of information on the printed page. Readers with a strong math background will be delighted; Goldberg's notation system is simple and consistent, and he usually explains the most important equations in words as well as symbols.

One of the book's most important features is a new system for graphical illustrations of wheel construction. (See figures and photo accompanying this review.) This includes both a side view and a "rim-edge" view, with a standard notation for indicating which spokes lace into the right and left flanges of the hub. Perhaps these graphics evolved through Goldberg's teaching experience, from the need for a simple way to draw complex wheel designs. In any case, it is a major contribution to the field. I would be happy to see this new graphical notation adopted by everyone who deals with wheelbuilding and design.

Goldberg aims his analytical lights at some areas of long-standing controversy: are radial spoking patterns really too stiff, and what is the best way to equalize the stresses in a dished wheel? He also breaks new ground by analyzing **asymmetric** spoking patterns (where the pulling spokes are laced in a different pattern than the non-pulling). I found his results intriguing, but I won't try to summarize them here, since I recommend that all wheelbuilders should read the book for themselves. But I can say that I would find Goldberg's arguments more convincing if he had carried out more empirical tests to verify his results. I suspect that a series of careful tests of wheel strength, spoke stress, hub size, spoking pattern, etc. would surprise everyone, at least slightly. Do I hear anyone volunteering to carry the tests out?

Still, most of Goldberg's suggested improvements do seem quite practical even without a sheaf of test measurements to back them up. For example, he recommends "forward rotation of the hub" to improve spoke life. This solution would require some re-engineering of most conventional hub designs. But at least one manufacturer of BMX hubs must be thinking the same way, since they have already incorporated this concept into their designs.

Most wheelbuilders have read Jobst Brandt's book **The Bicycle Wheel** (1983 revised edition available from Avocet, Inc., Menlo Park, CA). It's fair to say that Goldberg's book stands on the shoulders of Brandt's, even though Brandt is not mentioned once in it. Brandt, after all, was the first to apply the concepts of modern structural engineering to wheel design, and to report on his work so that others might learn. Now we have two good books, and still all the questions are not answered, at least to my mind. But I do recommend that wheelbuilders and budding wheel designers everywhere should have **both** books in their toolboxes.

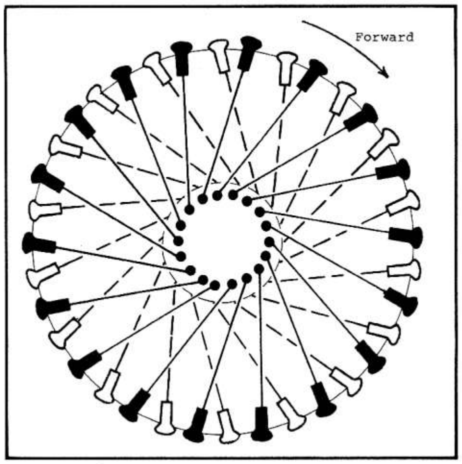

Right-side view of a 36-spoke dished rear wheel in which all right-side spokes (solid lines in foreground, with black nipples) are static, and all left-side spokes (dashed lines in background, with white nipples) are pulling. [Reprinted with permission.]

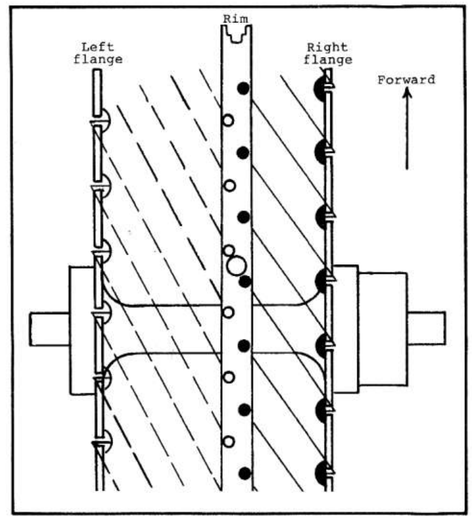

Edge view of a left-all pulling, right-all-static dished rear wheel. Proper valve location can be effected only with a left-hand rim. [Reprinted with permission.]

Excerpt from **The Spoking Word**

The major problems encountered in a conventional dished rear wheel are excessive tension in the right-pulling spokes and insufficient tension in the left-static spokes. The

A left-all-pulling, right-all-static wheel built around a special rear hub strengthened to resist the twist of one flange relative to the other. [Reprinted with permission.]

intensity of these problems may be reduced by:

(a) installing the right-side spokes in a more static direction, and

(b) installing the left-side spokes in a more pulling direction.

If we follow this idea to its logical conclusion, we come up with a wheel in which all right-side spokes are static and all left-side spokes are pulling. Spoking geometry for this wheel is shown in Figure L-8, and on the covers of this book. [Editor's note: Figure L-8 is reproduced to accompany this review.]

This wheel solves the two major problems associated with dished rear wheels (overloading of the right-pulling spokes and underloading of the left-static spokes) in the most simple and direct way possible. There simply are no right-pulling spokes or left-static spokes in this wheel.

Tension distribution in this wheel is very good. Tension in the spokes on the *right* side which, during steady-state is unavoidably higher than that on the left, is *reduced* during pulling. Conversely, tension in the spokes on the *left* side which, during steady-state is unavoidably lower than that on the right, is *increased* during pulling. Spoke tensions for this wheel are calculated in Appendix L-6.

Spoke angles u_L and u_R for this wheel must be selected with great care. The procedure leading to proper selection of these angles is explained in Appendix L-6. Typical values are $u_L = 82$ degrees, and $u_R = 38$ degrees. Once these angles are determined, proper spoke lengths can then be calculated from Eq. F-11. And finally, installing spokes of these lengths will guarantee that the spoke angles will actually conform to the calculated values and that the rim will be properly located between the two flanges and the hub.

One disadvantage of this spoking configuration is that it imposes an uncomfortably large twist (approximately 1875 in-lb. of torque in the steady-state condition) *across* the barrel of the hub. This torque comes about because all the spokes on the left are trying to rotate the left flange of the hub rearward, while all the spokes on the right side are trying to rotate the right flange of the hub forward. The resulting twist can easily demolish a hub of average strength. A strong disadvantage, but one that can certainly be overcome (see Photo L-8).

A second disadvantage of this wheel is that during pulling, tension increases in all the spokes on the left side and decreases in all the spokes on the right. As a result, the rim shifts to the left slightly during pulling. For the maximum probable load (200 lbs. bike-and-rider climbing a 10 degree hill), the rim shifts to the left about 0.1 inch. This could be a problem if the clearance between the rim and brake blocks, or that between the tire and chain stays, is small. A few ways of reducing the magnitude of this left-shift are suggested in Section L-31.

The main advantage of this wheel design is that the spokes will last almost forever. [Reprinted with permission.]

MATERIALS

Tests of Heat Treatment Effects in Brass-Brazed and TIG-Welded Lugless Joints

Keith Bontrager

Today's high-quality bicycle framesets are constructed using a variety of brazing and welding methods. "Lugless" frames are assembled using two techniques: *braze-welding,* where a low-melting temperature filler metal is added to the joint creating a fillet, and *welding,* where the joint is produced by melting the base metals at the joint and adding a steel filler material to produce the desired joint size and shape.

The heat used in all of these joining methods causes localized changes in the crystal structure and physical properties of the metal tubes of the frame. Roughly speaking, these "heat treatment" effects can be classified into two groups:

—"Annealing" represents a weakening of the tube: its tensile strength is decreased and its ductility (indicated by percent elongation at break) is increased. Annealing generally occurs when the tube is slowly cooled after brazing or welding.

—"Hardening" represents a strengthening of the tube: its tensile strength is increased, and its ductility is decreased. Hardening generally results from rapid cooling.

Previous work by Emiliani (Ref. 1) and Phelan and Cunningham (Ref. 2) pointed out how these heat treatment effects can be controlled by adjusting certain variables in the framebuilding process. In the tests reported here, I am concerned primarily with traditional brass-brazed lugless joints and how the amount of added filler metal affects the final tensile strength of the tube. For comparison, I also tested joints made by Tungsten Inert Gas (TIG) welding, an electric arc process currently used by several framebuilders. The results are in general agreement with the ideas of conventional metallurgy: joints with large amounts of filler metal cooled more slowly and caused greater annealing and weakening of the surrounding metal in the tube. Moreover, TIG welding produced a hardened, less ductile zone at the joint because of rapid cooling following the short, high-temperature welding process. These tests are the first reported efforts to quantify these effects in typical bicycle frame joints.

I used two popular brands of tubing in the tests: Reynolds 531, and Ishiwata "CrMo." These tubes have similar "as delivered" tensile strengths and other mechanical properties but show considerably different microstructures and ductile properties before brazing (Ref. 1).

Keith Bontrager is a professional framebuilder in Santa Cruz, CA.

The author expresses special thanks to R. Shafer, R. Lund, and C. Milazzo, Jr.

Brazing with Brass

Important variables in braze welding are the location where the weld is started, the time spent positioning the joint while brazing, the amount of filler metal added, and the rate of cooling. The brazing material (I used brass in these tests) will form a puddle at approximately 1620 to 1700°F, with temperatures decreasing in all directions away from the puddle. The thermal history of the tubes near the joint is quite complex because, as the brazing torch is moved around the work, the temperature alternates about the liquidus and solidus temperatures of the filler metal (Fig. 1). In any case, brazing invariably heats the tubing near the joint to temperature above its "austenitic transformation point." This is the temperature (approximately 1333°F) at which carbon steels undergo a major change in crystal structure: once the steel is heated above this temperature, its subsequent rate of cooling has a very critical effect on the final tensile strength and ductility of the material. On a microscopic level, it is likely that the heat of brazing causes most of the steel's carbide structure to diffuse into the austenitic phase; the end result, if the joint is cooled too slowly, will be "annealing" (hence weakening) of the tube.

Cooling rates for the braze welded joints I tested depend primarily on the amount of brass filler material that is used. The filler metal built up at the joint stores heat from the brazing operation. This heat is conducted down the tube and slows the cooling rate in the region near the joint. As the cooling rate is reduced, an annealed state can result in the tube, and the degree to which annealing has occurred determines the post-brazing strength of the tube near the joint. So, the longer the tubing and its joint take to cool, the softer is the tubing from more annealing.

We can relate the amount of filler metal (a difficult parameter to measure) to the radius of the fillet. Large radius fillets increase the mass of the brass filler by:

$$\Delta m(\%) = \rho \Delta V(\%) = 100\ ((r_2/r_1)^3 - 1)$$

Where:

Δm = increase in mass of filler metal
ρ = filler metal density
ΔV = filler metal volume change
r_2 = large radius
r_1 = small radius

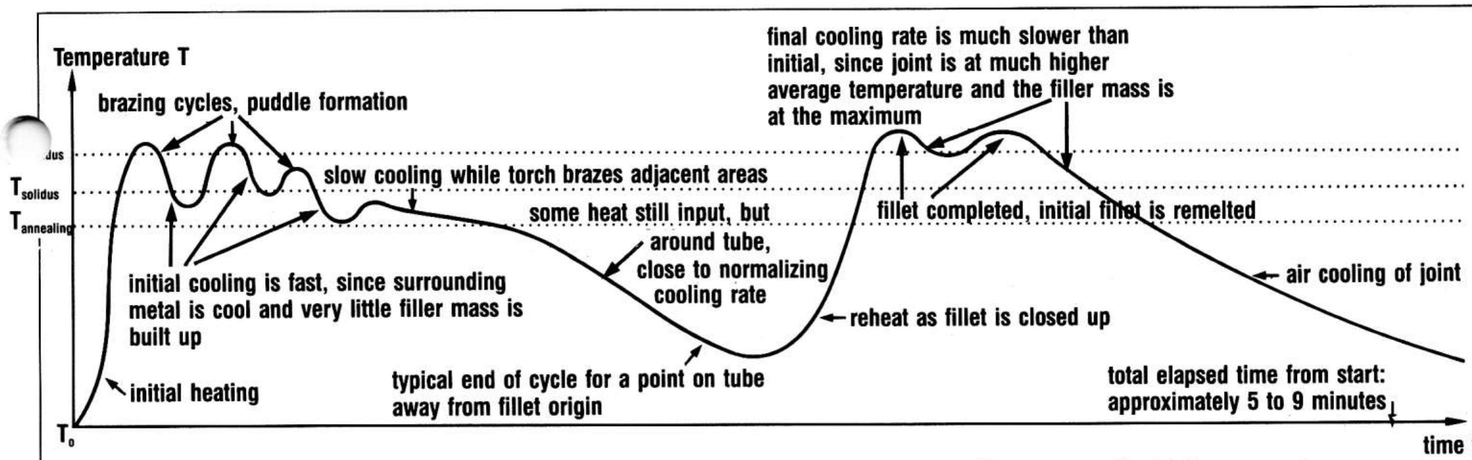

Figure 1: Anticipated time-vs.-temperature history for a fillet brazed joint, at the point where fillet starts on the joint.

Figure 2: Isotherms of Joint Samples (from oxide colors)

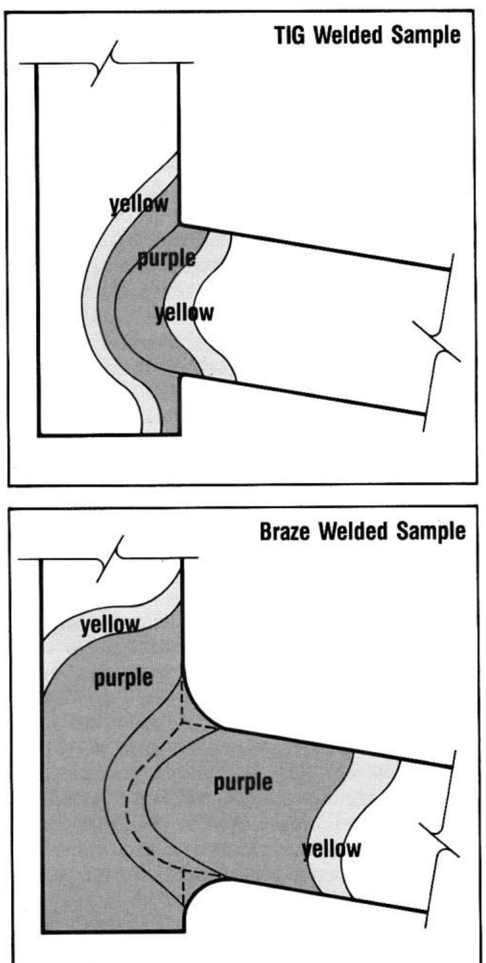

Figure 3: Structural changes in a single vee arc welded plate (from Ref. 5, page 281)

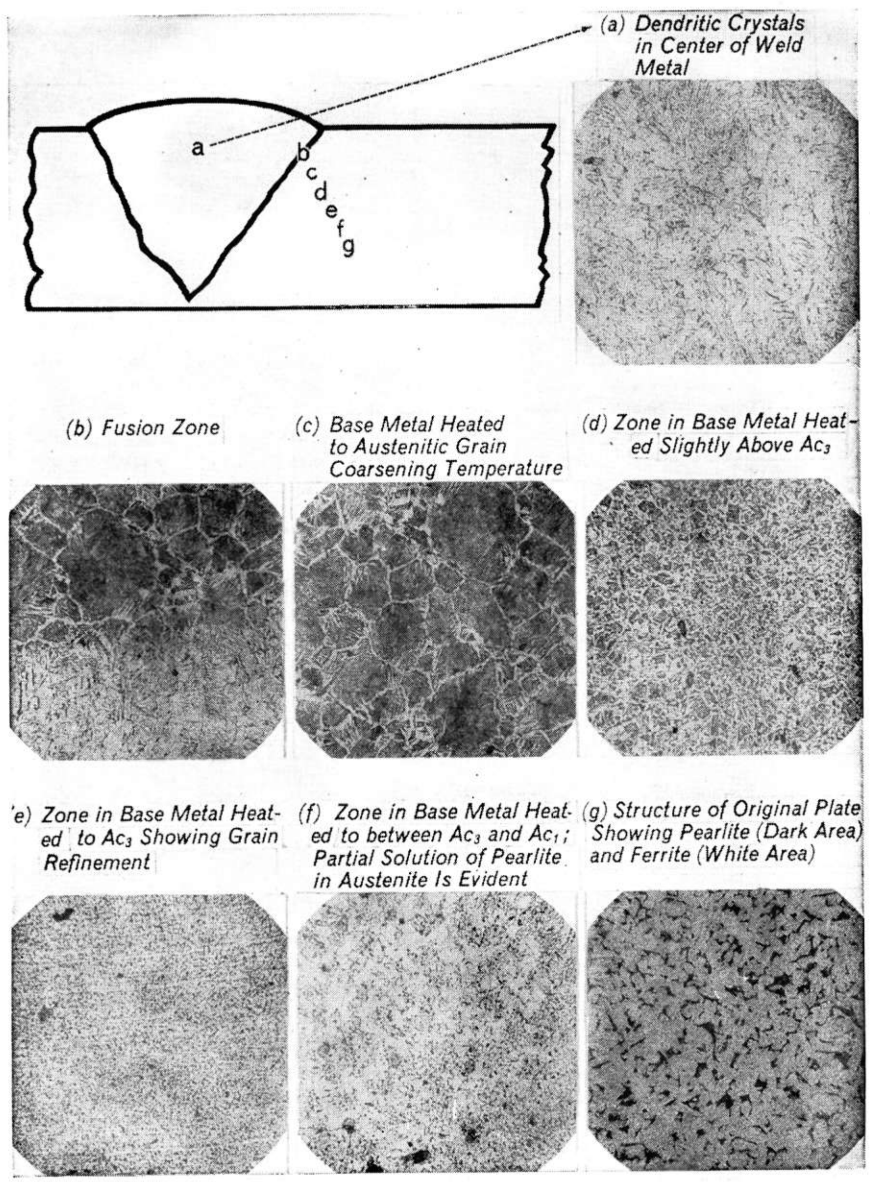

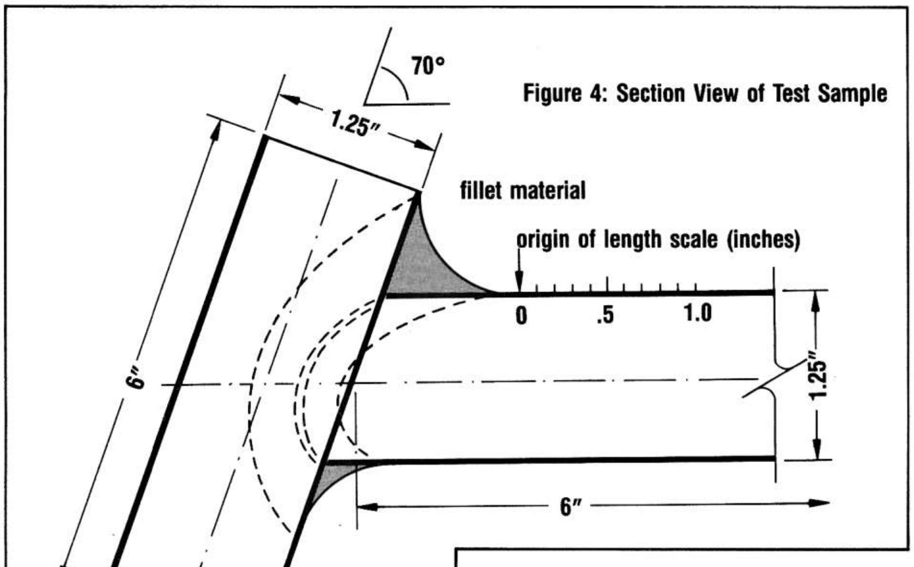

Figure 4: Section View of Test Sample

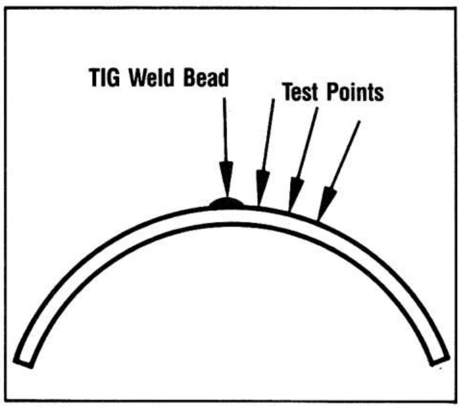

Figure 5: TIG Weld Bead on Unjoined Tube (Sample 12)

Figure 6: Diagram of test set up

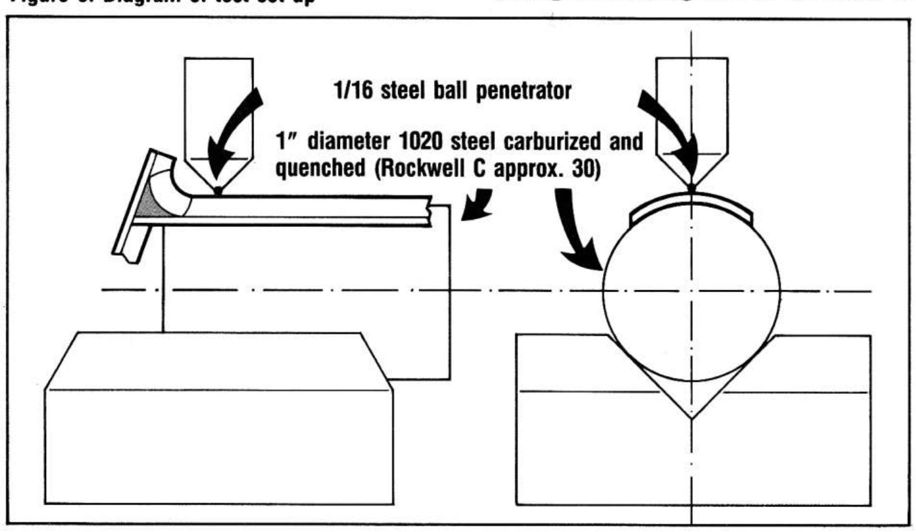

For example, the percent volume increase from this experiment's smallest radius (.10 inches) to the largest radius (.75 inches) sample is about 5,000 percent, or 50 times more brass.

Other effects on the cooling rate are the length of time the joint is at brazing temperature, and the section area of the tube available to conduct heat away from the joint. The heat conduction is directly proportional to the section area. The Ishiwata tube with a .040 inch wall has about 12 percent more section area than the .035 inch wall Reynolds tube, and should cool faster. A longer brazing time causes a slower cooling rate because additional heating of the joint raises the temperature of the tube adjacent to the joint, making the temperature gradient more gradual. Since the rate of cooling is proportional to this gradient, the tube cools more slowly if it is heated longer.

I estimated cooling rates by observing the colors of incandescence at the joint while brazing (Ref. 3, "Heat Treatment of Steel," page 1941). Although the actual colors varied with the brazing time, this rough estimate gave a cooling rate on the order of 40°F/sec for a medium size fillet. At this rate, partial transformation of the austenite should occur. Larger proportions of ferrite and/or pearlite and larger grain structures should be found in the slower cooled samples (Ref. 4). These structures will produce a weaker, more ductile tube. Conversely, quickly cooled samples should have less ferrite, smaller grain structures, and exhibit harder tubing near the joint.

TIG Metallurgy

In TIG welding, the electric field strength is sufficiently high to bring the metal to its melting temperature (2600°F) very quickly, about two to three seconds. Therefore, TIG welding times are very short compared to those of braze welding, and the heat-affected zone of the tubing is also correspondingly smaller, being localized to a region within .2 to .3 inches from the weld.

The small amount of heat required for TIG welding is demonstrated by the location of the oxide color bands on the tube after the weld (Fig. 2). The yellow band (approximately 450°F, see Ref. 3) is within 3/8 to 1/2 inch from the seam on the TIG welded samples, while the small fillet braze welded samples show this band 1 1/2 inches from the joint.

The puddle in a TIG welding joint also cools very quickly. Photomicrographs of the anticipated microstructures are shown in Fig. 3. The actual properties of the weld fillet are critical because the cooling rate can cause significant hardening and loss of ductility. Rough estimates of the average cooling rates (again, from observing the colors of the joint during welding) indicate that the joint material cooling rate is on the order of 300 to 400°F/sec, almost ten times faster than braze welding.

As a precaution against overhardening, it is common welding practice to use a mild steel filler (approximately .12 percent carbon). Since I have constructed bicycle frames with this filler material, I chose to use this technique for the TIG welded samples.

Preparing the Samples

Down tube joints were selected because they are prone to failure along the lines of Phelan and Cunningham's destructive test method (Ref. 2). My test specimens were mitered to simulate a common geometry used in off-road bicycles, and joined in a manner resembling the actual construction of this type of joint (Fig. 4). I decided on a six-inch tube length to provide sufficient thermal capacity and surface area to closely approximate the actual cooling rate of a frame assembly. (Later observations of oxide color band locations indicated that six inches was appropriate.)

All joints were brazed using standard production framebuilding techniques, including

Table 1: Test specimen identification and average measured hardness (Rockwell B).

Sample Number	Material	Joining Time (min)	Fillet Radius (inches)	Average measured hardness (Rockwell B) at specified distance (inches) from fillet edge (see Fig. 4) .0	.1	.2	.3	.4	.5	.6
1	I	9	.75	85.5	83.3	94.5	99	100	—	—
2	R	9	.50	86	89	90	96	98	—	—
3	I	5	.37	90	95	93	99	99	—	
4	R	6	.28	89	89.5	89	96	97	97	—
5	R&I	6	.21	96	95	95.5	94	95	98	—
6	I	6	.15	93.5	91	97	99	100	100	—
7	R	5	.10	97	95	92	97.5	100	100.5	100
8	R	3	TIG	100	97	97	98	97	—	—
9	I	3	TIG	101	99	98	100	100	100	100
10	R	tube "as delivered"		99 (control sample, not brazed)						
11	I	tube "as delivered"		98.5 (control sample, not brazed)						
12	R	TIG weld bead (Fig. 5)		see Table 2 for data						

I = Ishiwata "CrMo," R = Reynolds 531

control of the shape of the fillet in order to minimize finishing time. The time required to braze each joint was recorded, including the time required to reposition the tubes while brazing (See Table 1).

Strip samples of 1/2 inch width were cut from each brazed joint down the axis of the mitered (down) tube. These samples were taken from the section where the brass fillet build-up is largest, and where buckling failures noted by Phelan and Cunningham occur, corresponding to the underside of the down tube/head tube joint on a bicycle frame. The samples were cut out with a cold sawing procedure in order to avoid heat-treating them again. Care was taken to avoid bending the specimen at the joint to eliminate the possibility of strain hardening the sample. The TIG welded samples were prepared in the same way as the braze welded samples.

As control samples, strips of "as delivered" tube were prepared which were not subjected to any heat treatment (Samples #10 and #11). In addition, a non-joined tube (Sample 12) was prepared with a TIG weld applied along the tube axis (Fig. 5). This allowed a hardness test to be performed on the weld fillet itself.

Rockwell Testing

Hardness measurements were taken along the length of the sample strips using a Rockwell B hardness test (Fig. 6). None of the samples showed any marks from the indentor on the underside of the tube. As a rough guide, this indicates that the Rockwell B hardness scale was appropriate. At each point along the sample, several measurements were taken around the circumference and averaged. A larger spread in readings occurred in the area near the joint which was heat affected. The maximum speed in hardness measurements was three Rockwell B units, with one to two units' spread being typical. No correction was made for the shape of the specimens (cylindrical sections). This correction would raise the hardness values slightly, but would not alter the general results.

Hard Data

Table 1 shows the results of the hardness measurements down the length of the strip samples. I converted Rockwell hardness units to tensile strength units for graphing (Figs. 7 to 9) by using standard Rockwell conversion tables. As expected, joints with larger fillet radii (Samples 1, 2, and 3) showed a significant loss of strength at the joint because of annealing in the joint region. The Rockwell data suggest that strength differences on the order of 10 percent to 15 percent exist between the smallest and largest fillets. And I found that TIG welding produced less softening near the joint than braze welding, most likely from less annealing of the tube metal.

The graph in Fig. 7 shows the experimentally determined relationship of tensile strength and fillet radius. This relationship is linear throughout the radius range of most braze welds. The graphs in Figs. 8 and 9 show the comparison of strength vs. length away from the fillet edge; samples are grouped by tubing manufacturer. For both types of tubing, longer periods of braze welding combined with large radii fillets soften the region significantly within 0.4 inches from the edge of the fillet. TIG welded joints show much less softening in the heat affected zone (Samples 9 and 8 in Figs. 8 and 9, respectively). These joints had a much higher cooling rate than the braze welded samples.

Control Sample 12, prepared to examine the strength in the weld material, indicates that the weld material undergoes considerable hardening, even with the precautions taken by using mild steel filler metal. At a hardness of 110 Rockwell B, the material has a tensile strength of around 180 kpsi and ductility on the order of 6 percent elongation. In fact, the hardness measurement on Sample 12 may be lower than that of an actual welded joint because the amount of material available to conduct heat away from a puddle in this sample tube was reduced by 1/3 (no mitered tube, Fig. 5). The cooling rate would be faster on the sample joints.

Table 2: Average measured hardness (Rockwell B) of TIG weld bead

Distance (inches) from weld center	Hardness	Tensile Strength (kpsi)
0.0	110	180
0.1	103	130
0.2	93	90

Recommendations

My results show that the smallest possible brazed joint radius will produce the strongest joints by minimizing annealing effects. This applies to internally reinforced joints (Reg. 2) as well if the reinforcement dimensions are kept to a minimum.

In practice, the smallest brazeable fillet is on the order of .10 to .15 inch radius, due to the minimum area heated during brazing. A fillet of this size should provide adequate joint strength for a well-mitered unreinforced joint. Reinforced joints will require larger fillet radii.

One complication: the builder who is inexperienced with small radius fillets must pay more attention to fixture techniques. The strength of the brass filler at elevated tem-

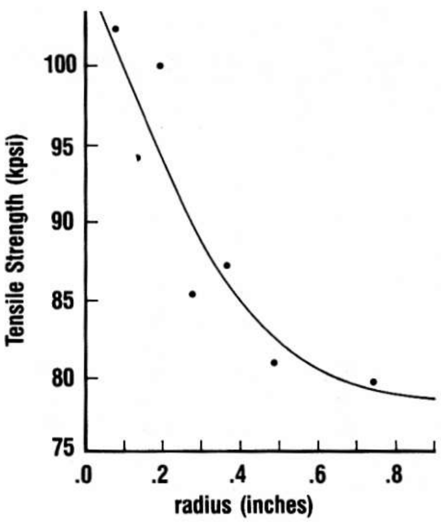

Figure 7: Strength at Joint vs. Fillet Radius for Braze Welded Samples

peratures is very low. Jigs and fixtures that constrain the tube in all directions can introduce stresses in the fillet that cause cracks in the filler, a result of the nonuniform expansion of the joint materials during heating. I have noticed this phenomenon when experimenting with fixture techniques.

Although TIG welding produces less annealing of the tubes than brazing, it introduces potential problems with brittle failures, and because of the geometry of the joint, it can cause stress concentrations which will lead to fatigue failures. The work of Phelan and Cunningham indicates that local reinforcement to reduce stress concentrations is a very effective way to increase the strength of the joint. This is true regardless of the method of construction.

TIG welding produces very localized heat affected zones. This characteristic can be used to produce "built-up" sections for reinforcement that shift the welded areas to relatively low stress areas of the tube. For example, a "saddle" gusset (Fig. 10) can be employed to move the welded zone around the tube to the neutral axis, minimizing the possibility of failure at the weld. This is not possible with brazing techniques because of the necessarily large heated area.

A TIG welded joint that includes one mild steel alloy tube (AISI #1010 or #1020), such as the bottom bracket joints of a bicycle frame, will be less prone to embrittlement during cooling since the material in the puddle will be lower carbon, less hardenable alloy. On tandem and off-road frames, the head tubes are often a very heavy gauge tube in order to eliminate distortion during the frame construction. These tubes could be an AISI 1020 tube rather than CrMo and still be adequately strong, and the resulting TIG welded joints would be less prone to the hardening effects as discussed above.

A simple unreinforced TIG welded butt joint has a very serious stress concentration in the joint when loaded in bending. Joint de-

Figure 8: Comparison of Ishiwata Samples

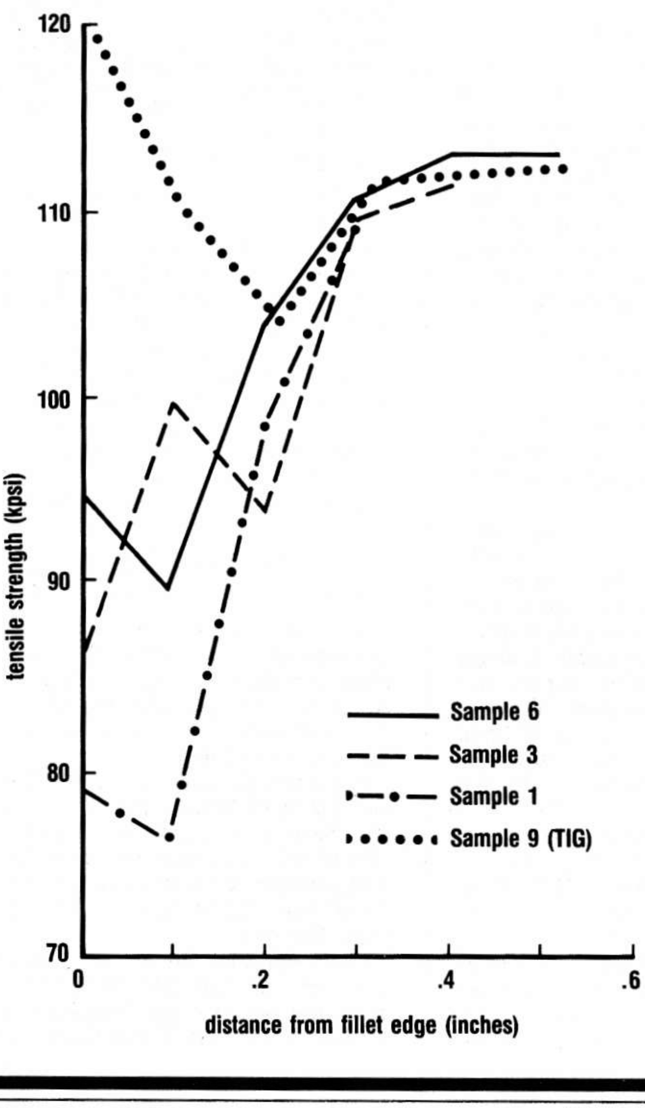

Figure 9: Comparison of Reynolds Samples

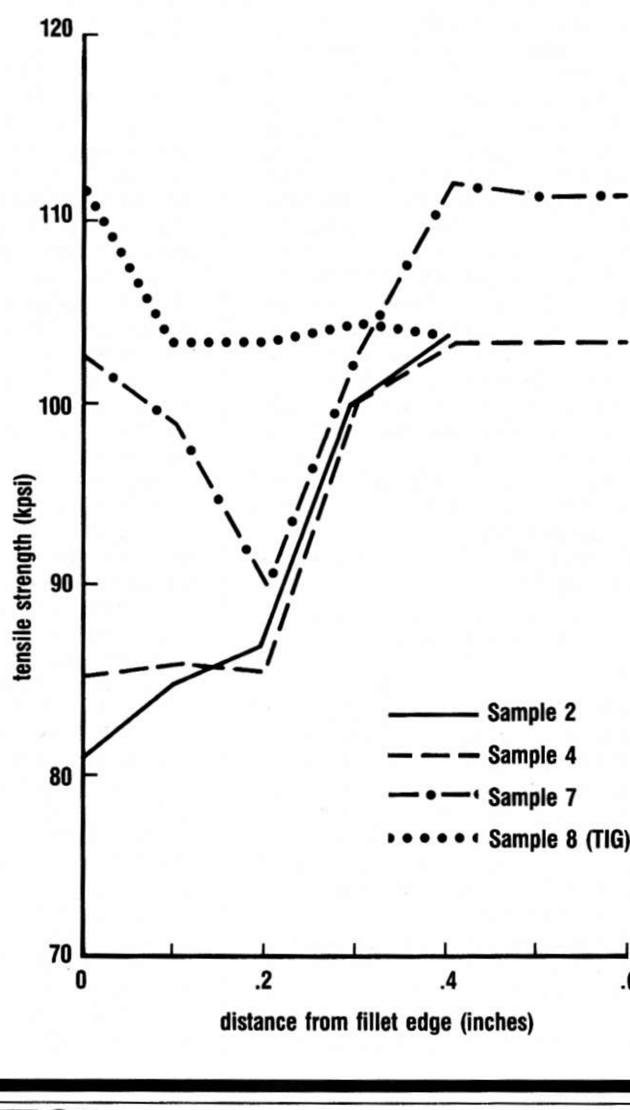

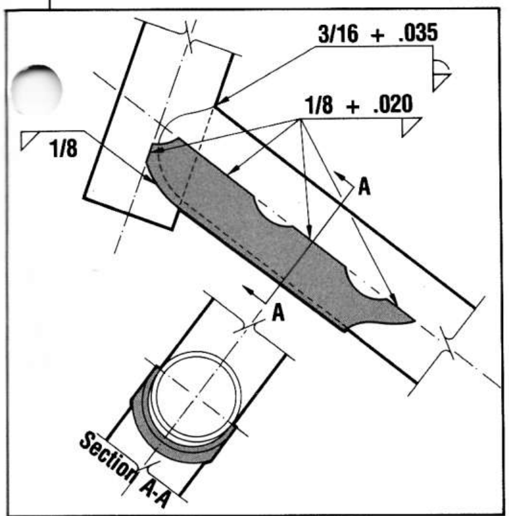

Figure 10: Diagram of "Saddle" Gusset

signs using light tube gauges must take this into account. The localization of the heat-treated metal at the joint makes this very important. Internal reinforcements, as discussed by Phelan and Cunningham are potentially useful in solving this problem.

A TIG welded joint can be purposely annealed or tempered after the weld has been completed, by heating with an oxy-acetalene torch. This step is mentioned by Reynolds Tube in their publication, "Guide to Cycle Questions." Often the assembly process can be designed to include this step while installing braze-ons in the area to be heat treated, eliminating the necessity of extra steps in the building process.

My personal observations indicate that the simplest (unreinforced) TIG welded frame may have adequate strength only for low stress applications. Severe off-road use can cause failures. There needs to be more qualitative work done on joint design and fatigue considerations.

Big is Not Beautiful

Since large radius fillets are so popular with some builders currently, we should reconsider the motivation behind this joining technique. The obvious reason for creating this sort of a joint would seem to be increased strength. Curiously, all of the builders with whom I have discussed this readily admit that a much smaller radius fillet will supply adequate strength. What then is the reason for this type of construction?

My experience indicates that brazed joints are built with large radius fillets for two reasons. The first is purely aesthetic. They look nice. Magazine writers have nice adjectives to describe them as well ("beefy," "massive," etc.).

The second is that they are *easy to "finish."* The finishing process involves smoothing out the irregularities along the surface of the fillet, and "blending" the weld into the tube. This is a demanding, time-consuming operation. Finishing is generally done with a hand-held rotary file using a "cartridge roll" abrasive cutter. The large fillets allow the use of a larger cartridge roll. The larger roll lasts longer, cuts faster at lower angular speeds that are easy to control, and allows the blending at the tube to be done with less risk of cutting away the tube wall. And, for a given volume of metal removed, the large roll will cut a shallower notch because of the smaller curvature at the cutting surface (larger radius).

The production of high quality braze welded frames is a labor-intensive process. Much of the time is spent in tedious finishing operations. So there is considerable incentive to produce an attractive product. But these tests indicate that large radii fillets, although perhaps more aesthetic and easier to produce, compromise the critical structural properties of the frame. These structural properties should take precedence if the frame is to be as strong and light as possible.

Future Study

Because of the complex thermal history of the brazed joints, a more statistically sound study is desirable. The average properties of a larger group of samples would smooth some of the fluctuations in the data. For example, Sample 7 yielded "as-delivered" hardness measurements above the rest of the group of Reynolds samples, and I noticed a spread in the hardness data around the periphery of the joints.

Though the as-delivered microstructures of the Ishiwata and Reynolds tubes are considerably different, it is probable that the heat treatment they receive during brazing would make them more similar after brazing. An examination of the microstructure before and after joining would allow a comparison of the effects of pre-brazing microstructure on the finished joints, if any.

Examining the microstructure in the heat affected zones of all specimens would reveal the nature of the heat treatment more accurately. In particular, examining the microstructure of the TIG welded samples for martensitic structures would be valuable.

References

1. "The Metallurgy of Brazing: Part 4," by Mario Emiliani; *Bike Tech,* Vol. 2, No. 2, April 1983.
2. "Calibrated Destructive Testing of Bicycle Frames," by Jacquie Phelan with Charles Cunningham; *Bike Tech,* Vol. 2, No. 4, August 1983.
3. *Machinery's Handbook* (19th edition), H. L. Horton, editor; Industrial Press, New York, NY; page 2060.
4. *Transformations in Metals,* by P. Shewmon, McGraw-Hill, New York, NY 1969.
5. *Metals and Plastics: Production and Processing,* by Thomas P. Hughes, Irwin-Farnham Co., Chicago, IL, 1948.

IDEAS & OPINIONS

Fork Tubing Dimensions

I enjoyed very much Ray Pipkin's Front Fork Analysis in August 1984 *Bike Tech.* But there is a mistake in it which results from misinterpreting the Columbus-SL specifications: the tubes used in making Columbus-SL fork blades do *not* have a uniform 0.91 mm thickness before tapering, as Pipkin assumes. Rather, they are a uniform 0.90 mm thick *after* tapering, according to both Columbus specifications and to measurements I took on a sample. Before tapering, they are single-butted tubes, with the wall thickness varying from 0.90 mm at the crown end to 0.45 mm at the dropout.

So some corrections in Pipkin's diagrams will be necessary. The graphs for Columbus-SL will always be parallel to those for Reynolds 531-SL. Actually, the Reynolds 531-SL is somewhat stiffer than Columbus-SL because of the thicker wall. Pipkin's diagrams showed the opposite.

This mistake is often made because Reynolds is the only manufacturer who specifies the wall thickness of fork blades *before* tapering. All other brands (Columbus, Ishiwata, Tange, Vitus) specify the wall thickness *after* tapering. This mistake appeared also in the "Straight Talk on Steel" article in July 1982 *Bicycling.*

Pipkin's graphs labeled Columbus-SL would actually apply to cheap "Hi-Ten" or low-carbon fork tubes, which are normally made from 1.2 mm thick unbutted tubing. It would be interesting to see the calculated flexibility results for such a fork tube.

Thomas Metzmacher
Munich, West Germany

Ray Pipkin responds:

I'm afraid I was the victim of advertising. The cleverly-worded ads for TI Reynolds suggested, without actually saying so, that *only* Reynolds' fork tubes have constant wall thickness after tapering. I took my data from *Delong's Guide to Bicycles and Bicycling,* Table 3.2, page 45, which reinforces the impression that Reynolds and Columbus forks differ in construction. In fact, Mr. Metzmacher is right: not only Reynolds and Columbus, but also the other manufacturers he mentions, produce fork tubes with constant wall thickness after tapering.

On the basis of this corrected data, I would agree that forks made of Columbus-SL and Reynolds 531-SL are nearly equivalent in stiffness, with the latter being slightly stiffer because of the thicker wall. Thanks to Thomas Metzmacher for setting the record straight.

newsline

TI REYNOLDS UPRATES 753 TUBING AND INTRODUCES NEW 500 SERIES: A 20% increase in the rated mechanical strength of Reynolds 753 frame tubes has been announced by TI Reynolds of Birmingham, England. The ultimate tensile strength rating has been improved to 179,200 psi (up from 168,000 psi), and the yield strength rating is now 156,800 psi. The fatigue strength rating has also been upgraded to 145,600 psi with up to two million stress-reversal cycles. According to Neal Kastley, TI Reynolds Marketing Manager, the upgrading was made possible by a new step in the proprietary production process (which already includes 7 cold-drawing operations and 11 heat-treatment cycles). The new treatment process uses vacuum induction furnaces manufactured by ABAR Corp. (of Ivyland, PA) which was recently bought out by Reynolds' parent corporation, Tube Investments, Ltd. Noting that 753 tubing was used in building two of the 1984 Olympic gold medal-winning bicycles, Kastley points out that the upgraded 753 tubing will provide a 20% improvement in frame strength and fatigue resistance.

In a separate announcement, TI Reynolds has introduced the new "500" series of chrome-molybdenium alloy main frame tubes. The 500 series tubes are based on the well-known Reynolds 501 Cromalloy-M specification, but have a constant wall thickness (20 gauge), and a rated tensile strength of 98,600 psi. Reynolds is targeting the new 500 series at the high-volume manufacturers of conventional lightweight sports bikes and BMX machines.

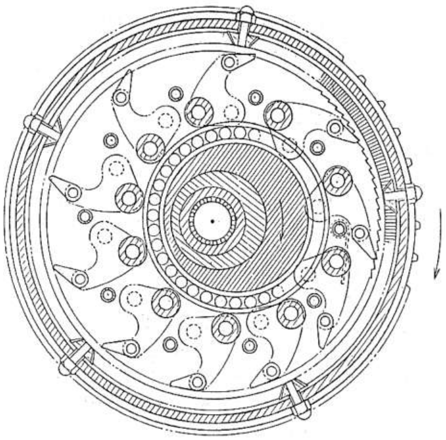

BRIDGESTONE UNVEILS NEW STEPLESS TRANSMISSION: A continuously variable transmission that mounts on the crank axle, in place of chainwheels, has been introduced by Bridgestone in the US and Europe. Full details of how the mechanism works have not yet been released, but drawings provided to *Bike Tech* by Bridgestone show that the system uses an eccentric rotor to drive a series of ten ratchet-and-pawl arms (see illustration). The system seems to work well: the demonstration model shown last October at the Las Vegas Interbike Show did indeed give stepless shifting over a wide ratio range. Stay tuned for further details.

DESIGN COMPETITION FOR NEIGHBORHOOD BICYCLE SHELTERS IN NEW YORK CITY: The Stryker's Bay Neighborhood Council, of the Upper West Side of Manhattan, is looking for innovative designs for overnight bicycle shelters. There are an estimated two and one-half million bicycles in New York City, yet most residents have no reasonably secure and convenient means for parking their vehicles. To help remedy the problem, the Neighborhood Council is sponsoring a Design Competition which will award $1200, $600, and $300 prizes to the designs judged to be most "economical, street-wise, and appealing." The judging panel will include representatives of local bike shops, cycling advocacy groups, architectural and industrial designers, and the police department. To enter the competition, designers must first register by sending $15 along with their name, address, and phone number to: "Bicycle Shelter Design Competition," Stryker's Bay Neighborhood Council, 561 Columbus Ave., New York, NY 10024. Deadline for registrations is March 22, 1985; deadline for submissions is April 22, 1985.

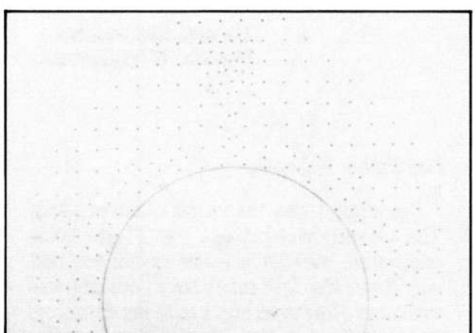

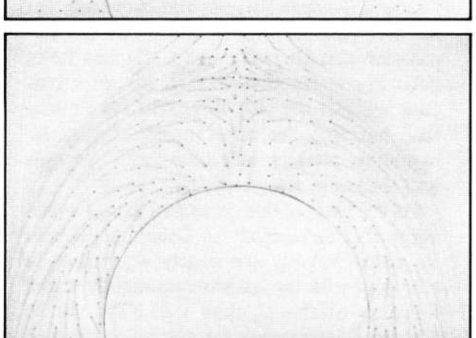

Photos courtesy NASA Lewis Research Center

NEW FLOW VISUALIZATION TECHNIQUE REVEALS SURFACE STREAMLINES: Flow visualization is an experimental technique used extensively in the aerodynamic design of aircraft and automobiles. The technique could help designers of bicycles and HPV's in their efforts to reduce air drag. But the complexity and expense of the procedure has limited its use to high-budget projects. Now, however, a new flow visualization method has been developed that is simple and inexpensive enough to be useful to experimenters and inventors in the cycling world.

The new technique provides a permenent record of ink traces that reveal the shape and direction of flow streamlines near a solid surface. First, a matrix of ink-dots is applied to matte polyester drafting film using an indelible felt-tip pen (see upper illustration). Then the film is attached to the surface of interest (eg, a fairing). Finally, a layer of Oil of Wintergreen (methyl salicylate) is sprayed onto the film, and the air flow (from fan, wind tunnel, or forward motion) is started. The result is that the ink dots slowly "dissolve" into the Oil of Wintergreen, which is being swept along the surface in the dominant pattern of flow. After a few minutes, the Oil has evaporated, leaving a permanent picture of ink traces that reveal the streamlines of flow near the surface (see lower illustration, which shows the classical flow pattern around a circular cylinder). A knowledgeable designer can interpret these patterns to find clues for reducing air drag.

Further details are given in the report "A New Surface-Streamline Flow Visualization Technique," by L.S. Langston and M.T. Boyle, *Journal of Fluid Mechanics, 125*, pp. 53-57, and in Technical Support Package #LEW-13875, available free from NASA, P.O. Box 8757, Baltimore-Washington International Airport, MD 21240.